

# Highly Branched RG-I Domain Enrichment Is Indispensable for Pectin Mitigating against High-Fat Diet-Induced Obesity

Kai Zhu, Guizhu Mao, Dongmei Wu, Chengxiao Yu, Huan Cheng, Hang Xiao, Xingqian Ye, Robert J. Linhardt, Caroline Orfila, and Shiguo Chen\*

 Cite This: *J. Agric. Food Chem.* 2020, 68, 8688–8701

 Read Online

ACCESS |

 Metrics & More

 Article Recommendations

 Supporting Information

**ABSTRACT:** Obesity is associated with gut microbiome dysbiosis. Our previous research has shown that highly branched rhamnogalacturonan type I (RG-I)-enriched pectin (WRP, 531.5 kDa, 70.44% RG-I, Rha/(Gal + Ara) = 20) and its oligosaccharide with less branched RG-I [DWRP, 12.1 kDa, 50.29% RG-I, Rha/(Gal + Ara) = 6] are potential prebiotics. The present study is conducted to uncover the impact of the content, molecular size, and branch degrees of RG-I on the inhibiting effect of high-fat diet (HFD)-induced obesity. The commercial pectin (CP, 496.2 kDa, 35.77% RG-I, Rha/(Gal + Ara) = 6), WRP, and DWRP were orally administered to HFD-fed C57BL/6J mice (100 mg kg<sup>-1</sup> d<sup>-1</sup>) to determine their individual effects on obesity. WRP significantly prevented bodyweight gain, insulin resistance, and inflammatory responses in HFD-fed mice. No obvious anti-obesity effect was observed in either CP or DWRP supplementation. A mechanistic study revealed that CP and DWRP could not enhance the diversity of gut microbiota, while WRP treatment positively modulated the gut microbiota of obese mice by increasing the abundance of *Butyrivibrio*, *Roseburia*, *Barnesiella*, *Flavonifractor*, *Acetivibrio*, and *Clostridium* cluster IV. Furthermore, WRP significantly promoted browning of white adipose tissues in HFD-fed mice, while CP and DWRP did not. WRP can attenuate the HFD-induced obesity by modulation of gut microbiota and lipid metabolism. Highly branched RG-I domain enrichment is essential for pectin mitigating against the HFD-induced obesity.

**KEYWORDS:** RG-I, molecular weight, side chain, pectin, high-fat diet, obesity, gut microbiota

## 1. INTRODUCTION

The prevention of obesity is a challenge of global proposition. Evidence has shown that obesity is associated with reduced gut bacterial diversity or altered proportions of bacterial species.<sup>1–4</sup> Consumption of plant polysaccharides revealed a significant and positive effect on adiposity-induced lipid metabolic disorders and gut microbiota dysbiosis.<sup>5–8</sup> Among them, pectin and derived-oligosaccharides are good candidate modulators of obesity because of their fermentation potential by various probiotic microorganisms to modulate the obesity due to their complex structure that are fermented by various of probiotics.<sup>9–11</sup>

Pectin is a complex heteropolysaccharide which consists of structurally distinct domains including homogalacturonan (HG), xylogalacturonan, rhamnogalacturonan type I (RG-I), rhamnogalacturonan type II (RG-II), arabinan, and arabinogalactan. RG-I is composed of a backbone being formed from a repeating disaccharide of [→2)-α-L-Rhap-(1 → 4)-α-D-GalAp-(1→] residues with Ara and Gal residues attached to the O-4 or O-3 position of α-L-Rhap backbone units.<sup>12,13</sup> It is usually removed from commercial pectin (CP) preparations by hot acid treatment as it is considered a hindrance for pectin gelling.<sup>14,15</sup> However, accumulating evidence has demonstrated that pectin containing RG-I regions from various sources can modulate the composition of obesity-related intestinal microbiota and increase the production of butyrate, which is a dominant protective agent against obesity.<sup>16–20</sup> Recent findings suggested have reported that polysaccharide utilization

loci of gut bacteria activated by different RG-I domains can recruit a myriad of glycoside hydrolases (GHs) and polysaccharides lyases for metabolism of RG-I pectin molecules.<sup>21,22</sup> Thus, RG-I is hypothesized to contribute significantly to bacterial fermentation in the colon, leading to favorable changes in gut microbiota composition.<sup>23,24</sup> Particularly, Khodaei and his colleagues have confirmed that potato RG-I pectin stimulated the growth of *Lactobacillus* spp. and *Bifidobacterium* spp. Reduction in these two species are proposed to be a biomarker of gut dysbiosis and found to be decreased under high-fat diet (HFD) conditions.<sup>25</sup> A recent research also indicated that the pectin-containing RG-I can modulate the composition of obesity-related gut microbiota and upregulate the production of butyrate—a dominant protective agent against obesity.<sup>26</sup> Moreover, apple pectin rich in RG-I strongly promoted *Bifidobacterium*, *Bacteroides*, and *Lactobacillus* in HFD-fed mice colon, subsequently producing short-chain fatty acids (SCFAs), which limited the secretion of proinflammatory cytokines and alleviated the obesity-caused inflammation.<sup>27</sup> However, until now, the impact

Received: April 27, 2020

Revised: June 2, 2020

Accepted: July 7, 2020

Published: July 7, 2020



of RG-I content in pectin on HFD-induced obesity is still unclear.

Apart from the RG-I content, another factor that affected the bioactivity of RG-I pectin is molecular size.<sup>28</sup> A recent study on citrus pectic oligosaccharides containing RG-I with a molecular weight of 3–4 kDa has shown hypocholesterolemic effects on HFD-fed mice by modulating specific gut bacterial groups.<sup>10</sup> Besides, the report from Gómez et al. has shown that pectic oligosaccharides (5.9–22.8 kDa) containing relative high content RG-I (37.65%) caused better shifts in prebiotic properties than high  $M_w$  pectin (51.4–82 kDa), confirming the significance of molecular size in functional properties of RG-I pectin.<sup>29</sup> However, most of the research merely focused on the preparation and probiotic effect of pectic oligosaccharides that primarily consisted of HG, and less studies were conducted on RG-I-enriched oligosaccharides.<sup>11,29,30</sup> Furthermore, a greater proportion of side chains in RG-I pectin that can promote the growth of *Bacteroides* species was confirmed.<sup>31–33</sup> The arabino/galacto-oligosaccharides derived from the side chains of RG-I were proved to be highly fermented by *Bifidobacterium* than those from the backbone of RG-I.<sup>25</sup> These observations indicate that the neutral sugar branching chains may have a great impact on the gut microbial composition improvement of RG-I-enriched oligosaccharides because the neutral sugar side chains were degraded significantly during the pectic oligosaccharide preparation process. It is also necessary to take the branching degrees into account for the assessment of the RG-I oligosaccharide beneficial effects in the gut microbiota.

In our previous study, RG-I-enriched oligosaccharides [DWRP, 50.29% RG-I content, 12.1 kDa, Rha/(Gal + Ara) = 1:6] degraded from citrus canning processing basic water recovered pectin [WRP, 70.44% RG-I, 531.5 kDa, Rha/(Gal + Ara) = 1:20] were obtained by metal-free Fenton reaction.<sup>34</sup> DWRP can significantly enrich *Bifidobacterium* and *Lactobacillus* populations, and WRP can improve *Bacteroides*, *Desulfovibrio*, and *Ruminococcaceae* in mice.<sup>29</sup> The results evidenced that both the highly branched RG-I enriched pectin with large  $M_w$  and RG-I oligosaccharides with less branching degree can modulate the gut microbiota. However, these effects on gut microbes of obesity mouse are still unclear.

Therefore, the main aim of this study was to uncover the contribution of RG-I content, molecular size, and branching degrees of pectin on the alleviation of HFD-induced obesity and obesity-induced microbiota dysbiosis shaping. The RG-I-enriched pectin recovered (WRP), its degradation products (DWRP), and commercial HG-dominated pectin [CP, 496.2 kDa, 35.77% RG-I, Rha/(Gal + Ara) = 6] were selected in this study. First, the effects of CP, WRP, and DWRP treatment on obesity and obesity-induced metabolic disorders in HFD-fed mice were investigated. Then, the contribution of pectin on gut microbiota composition and SCFAs was studied by 16S rRNA and gas chromatography. Moreover, quantitative real-time-polymerase chain reaction (qRT-PCR) analysis and immunohistochemistry were also used to analyze the expression of genes and proteins related to brown-like adipocyte formation, respectively.

## 2. EXPERIMENTAL SECTION

**2.1. Preparation of Pectin.** Rhamnogalacturonan-I (RG-I)-enriched pectin (WRP) and its degradation products (DWRP) were recovered from citrus (*Citrus unshiu* Marc.) processing water by sequential acid and alkaline treatments in a previous study.<sup>35</sup> WRP

( $M_w$  = 531.5 kDa) was recovered from the citrus segments material and was previously reported to have 70.44% of RG-I content with a high degree of side chain branching [Rha/(Gal + Ara) = 1:20], while its depolymerized fraction DWRP ( $M_w$  = 12.1 kDa, 56.29% RG-I content) with less side chain branching [Rha/(Gal + Ara) = 1:6]. CP was bought from Sigma-Aldrich (Shanghai, China) and is mainly composed of HG (52.55%) with an average  $M_w$  of 496.2 kDa, and a low degree of side chain branching [Rha/(Gal + Ara) = 1:6] was used in the present study.

**2.2. Animal Experiments.** Fifty C57BL/6J male mice (SPF, 6–8 weeks old, IACUC-20180917-02) were kept under specific-pathogen-free conditions in a 12 h light/dark cycle with free access to standard chow diet (CD; 12% of energy from fat; Rodent diet, SHOBREE, Jiangsu Synergy Pharmaceutical Biological Engineering Co., Ltd., Nanjing China) and sterile drinking water in a temperature-controlled room ( $21 \pm 2$  °C). After an accommodation period of 1 week, the mice were randomly divided into five groups (10 mice/group) and were fed for 8 weeks with CD, (HFD, 60% of energy from fat; Research Diets D12492, Open Source Diets, USA), HFD with 100 mg/kg CP (HFD-CP), HFD with 100 mg/kg WRP (HFD-WRP), and HFD with 100 mg/kg DWRP (HFD-DWRP). A certain amount of pectin according to the dosages of 100 mg/kg was dissolved in 200  $\mu$ L of distilled water and administrated orally via intragastric gavage once per day. The compositions and energy densities of the diets are listed in Table S1. Body weight and food intake were measured weekly.

The oral glucose tolerance test (OGTT) was performed three days before sacrifice. Overnight-fasted mice were administrated with glucose solution (2 g/kg body weight, 66% solution) by oral gavage; then, blood glucose was measured from tail vein blood at 0, 30, 60, 90, and 120 min using test strips (ACCU-CHEK Performa) and a portable glucose meter (Roche Diagnostics, Shanghai, China). The blood glucose level before glucose administration represented the fasting glucose concentration. Incremental area under the curve (AUC) was calculated using the trapezoidal method.

Mice were fasting for 12 h, anaesthetized, and sacrificed by cervical dislocation after 9 weeks. Blood and tissues were collected and stored at  $-80$  °C until further use. All procedures were approved by the Institutional Animal Care and Use Committee of Zhejiang University School of Medicine.

**2.3. Biochemical Analysis and Cytokine Measurements of Serum.** Serum was isolated by centrifugation (4 °C, 12,000g, 10 min). Serum total cholesterol (TC), triglycerides (TG), high-density lipoprotein cholesterol (HDL-C), and low-density lipoprotein cholesterol (LDL-C) were measured using commercial kits (Nanjing Jiancheng Bioengineering Institute, Nanjing, China) according to the manufacturer's instructions. Serum TNF- $\alpha$ , IL-6, lipopolysaccharide (LPS), insulin, and adiponectin protein levels were then quantified using commercial ELISA kits (Cloud-Clone Crop., USA) following the manufacturer's instruction.

**2.4. Liver and Epididymal Fat Histology.** The fresh liver, inguinal white adipose tissue (iWAT), and epididymis WAT (eWAT) were isolated and fixed with 4% neutral formalin solution at room temperature for 48 h. After dehydration, eWAT, iWAT, and liver were clarified in benzene and embedded in low melting point paraffin wax. Sections (3 nm thick) were cut and stained with haematoxylin and eosin (H&E staining) for light microscopic examination. All of these assays were performed in a blinded manner.

**2.5. Immunohistochemistry Staining.** The paraffin sections of iWAT were subjected to deparaffination, antigen retrieval, and endogenous peroxidase activity blocking. Thereafter, slides were incubated with uncoupling protein 1 (UCP1) primary antibody (Santa Cruz Biotechnology Inc., USA) and horseradish peroxidase-conjugated secondary antibody. After 3,3'-diaminobenzidine immunostaining, harris hematoxylin counterstaining, dehydration, and coverslipping, the sections were observed in a DS-R1-U3 Nikon digital imaging system and the positive integral optical density of UCP1 in the immunohistochemical pictures was analyzed with ImageJ software (National Institute of Health, MD, USA).

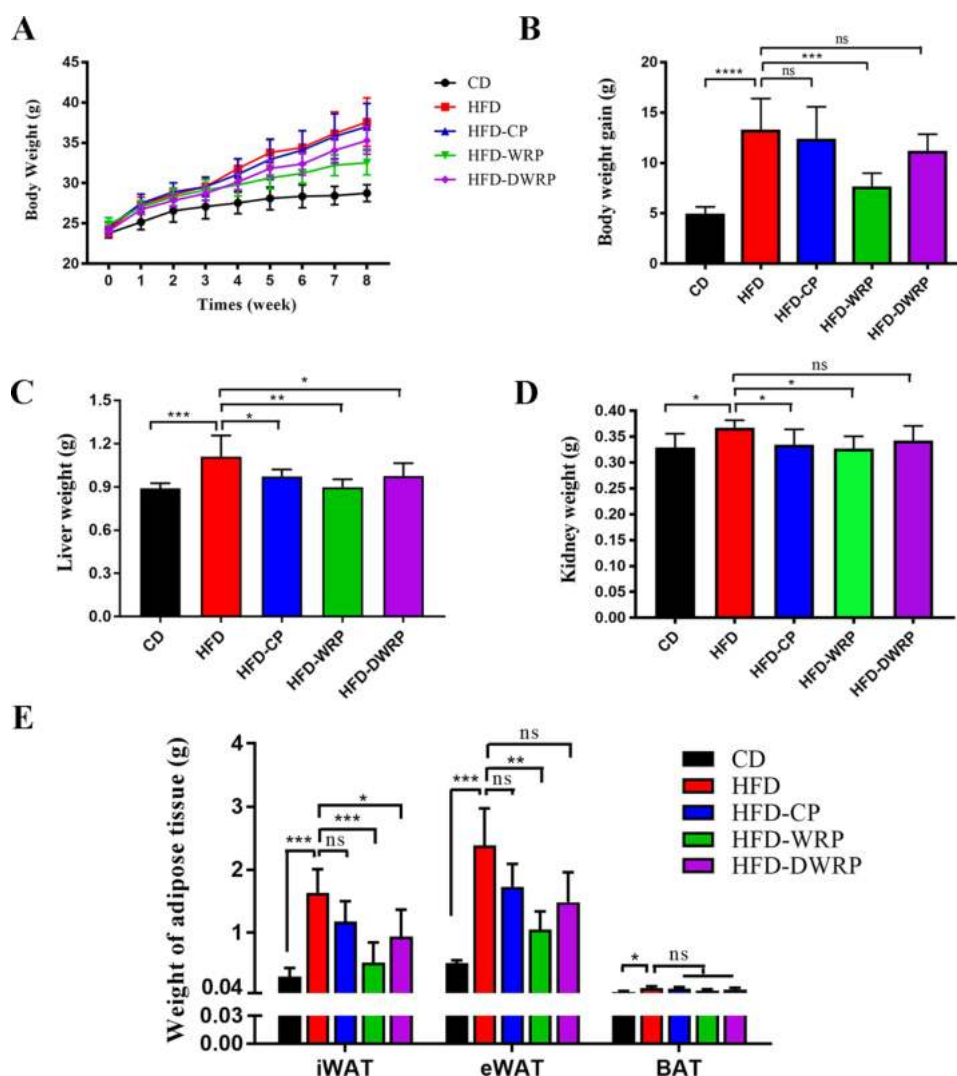


**Figure 1.** Whole body and tissue weight fed on conventional chow (CD) and HFD for 8 weeks. (A) Growth curve of mice in different groups; (B) weight gain of mice in each group after 8 weeks of feeding; (C–E) shows the weight of liver, kidney, iWAT, epididymal white adipose tissue and brown adipose tissue of mice. [Data are presented as means  $\pm$  SD ( $n = 8$  mice per group), \* $p < 0.05$ ; \*\* $p < 0.01$ ; \*\*\* $p < 0.001$ ; and \*\*\*\* $p < 0.0001$ ; ns, not significant].

**2.6. RNA Extraction and qRT-PCR Analysis.** Total RNA was extracted from eWAT, iWAT, and BAT using TRIzol reagent (Invitrogen, CA, USA), which was then used to synthesize cDNA with PrimeScript RT reagent kit with gDNA Eraser (Takara, Beijing, China). qRT-PCR was performed using SYBR Green Master Mix (Applied Biosystems, CA, USA), 96-well plates, and an Applied Biosystems QuantStudio 3 Real-Time PCR instrument (Life Technologies, Singapore). qPCR was performed for 40 cycles with following programs: 50 °C for 2 min, 95 °C for 1 s, and 60 °C for 40 s. Relative quantification was done based on the  $2^{-\Delta\Delta Ct}$  method. Expression was normalized to the housekeeping gene.

**2.7. 16S rRNA Gene Analysis.** Cecal samples were collected and used for bacterial 16S rRNA sequencing. Five samples of each group were selected randomly for 16S rRNA analysis. DNA was extracted from the cecal solid contents of mice by using the E.Z.N.A. Stool DNA Kit (D4015, Omega, Inc., USA) according to manufacturer's instructions. The total DNA was eluted in 50  $\mu$ L of elution buffer and stored at  $-80$  °C until measurement in the PCR by LC-Bio Technology Co., Ltd. The V3–V4 region of the prokaryotic (bacterial

and archaeal) small-subunit (16S) rRNA gene was amplified with slightly modified versions of primers 338F (5'-ACTCCTACGG-GAGCAGCAG-3') and 806R (5'-GGACTACHVGGGTWTC-TAAT-3').<sup>36</sup> The 5' ends of the primers were tagged with specific barcodes per sample and sequencing universal primers.

The PCR products were purified by AMPure XT beads (Beckman Coulter Genomics, Danvers, MA, USA) and quantified by Qubit (Invitrogen, USA). The amplicon pools were prepared for sequencing, and the size and quantity of the amplicon library were assessed on Agilent 2100 Bioanalyzer (Agilent, USA) and with the Library Quantification Kit for Illumina (Kapa Biosciences, Woburn, MA, USA), respectively. PhiX Control library (v3) (Illumina) was combined with the amplicon library (expected at 30%). The libraries were sequenced on 300PE MiSeq runs, and one library was sequenced with both protocols using the standard Illumina sequencing primers, eliminating the need for a third (or fourth) index read.

Samples were sequenced on an Illumina MiSeq platform according to the manufacturer's recommendations, provided by LC-Bio. Paired-end reads were assigned to samples based on their unique barcode

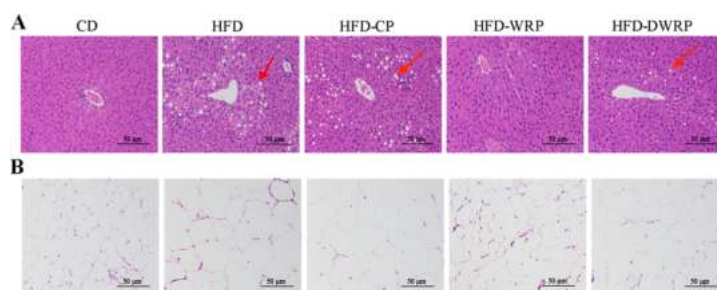


**Figure 2.** Histological assessment of livers (A) and epididymal white adipose tissue (B) in HFD-induced obesity mice. (H&E stain, 200 $\times$  magnification).

**Table 1.** Effects of RG-I pectin on serum Biochemical Parameters in C57BL/6 Mice<sup>a</sup>

groups	CD	HFD	HFD-CP	HFD-WRP	HFD-DWRP
TC (mmol/L)	4.99 $\pm$ 0.65 <sup>a</sup>	9.66 $\pm$ 0.75 <sup>d</sup>	8.58 $\pm$ 0.76 <sup>c</sup>	5.28 $\pm$ 0.42 <sup>a</sup>	6.43 $\pm$ 0.56 <sup>b</sup>
TG (mmol/L)	1.15 $\pm$ 0.27 <sup>a</sup>	1.49 $\pm$ 0.11 <sup>b</sup>	1.41 $\pm$ 0.21 <sup>ab</sup>	1.26 $\pm$ 0.30 <sup>ab</sup>	1.27 $\pm$ 0.15 <sup>ab</sup>
HDL-C (mmol/L)	1.52 $\pm$ 0.27 <sup>a</sup>	2.10 $\pm$ 0.37 <sup>ab</sup>	2.12 $\pm$ 1.02 <sup>bc</sup>	2.65 $\pm$ 0.62 <sup>c</sup>	2.81 $\pm$ 1.47 <sup>c</sup>
LDL-C (mmol/L)	1.99 $\pm$ 0.45 <sup>a</sup>	4.00 $\pm$ 1.78 <sup>b</sup>	2.94 $\pm$ 0.39 <sup>a</sup>	2.01 $\pm$ 0.54 <sup>a</sup>	2.29 $\pm$ 0.77 <sup>a</sup>
FFA (mmol/L)	1.27 $\pm$ 0.43 <sup>ab</sup>	1.72 $\pm$ 0.12 <sup>b</sup>	1.57 $\pm$ 0.47 <sup>b</sup>	1.33 $\pm$ 0.33 <sup>ab</sup>	1.20 $\pm$ 0.44 <sup>a</sup>
insulin (ng/mL)	0.38 $\pm$ 0.12 <sup>a</sup>	0.76 $\pm$ 0.27 <sup>c</sup>	0.61 $\pm$ 0.19 <sup>bc</sup>	0.50 $\pm$ 0.20 <sup>ab</sup>	0.56 $\pm$ 0.15 <sup>ab</sup>
LPS (EU/mL)	0.44 $\pm$ 0.02 <sup>ab</sup>	0.54 $\pm$ 0.05 <sup>c</sup>	0.54 $\pm$ 0.14 <sup>bc</sup>	0.41 $\pm$ 0.07 <sup>a</sup>	0.39 $\pm$ 0.07 <sup>a</sup>
TNF- $\alpha$ (ng/mL)	1.29 $\pm$ 0.55 <sup>bc</sup>	1.58 $\pm$ 0.35 <sup>c</sup>	0.91 $\pm$ 0.39 <sup>ab</sup>	0.68 $\pm$ 0.19 <sup>ab</sup>	0.52 $\pm$ 0.12 <sup>a</sup>
adiponectin ( $\mu$ g/mL)	51.03 $\pm$ 12.95 <sup>d</sup>	27.14 $\pm$ 3.62 <sup>a</sup>	31.52 $\pm$ 3.54 <sup>ab</sup>	47.77 $\pm$ 9.45 <sup>cd</sup>	38.07 $\pm$ 4.36 <sup>bc</sup>
TG/HDL-C	0.74 $\pm$ 0.24 <sup>a</sup>	0.75 $\pm$ 0.14 <sup>a</sup>	1.33 $\pm$ 1.25 <sup>a</sup>	0.48 $\pm$ 0.05 <sup>a</sup>	0.55 $\pm$ 0.19 <sup>a</sup>
HDL-C/LDL-C	0.78 $\pm$ 0.11 <sup>a</sup>	0.57 $\pm$ 0.22 <sup>a</sup>	0.63 $\pm$ 0.33 <sup>a</sup>	1.38 $\pm$ 0.43 <sup>b</sup>	1.54 $\pm$ 1.19 <sup>b</sup>

<sup>a</sup>The means with different superscript letters (a, b, and c) represent statistically significant results ( $p < 0.05$ ) based on ANOVA with Duncan's range tests, whereas means labeled with the same superscript correspond to results that show no statistically significant differences.

and truncated by cutting off the barcode and primer sequence. Paired-end reads were merged using FLASH. Quality filtering on the raw tags was performed under specific filtering conditions to obtain the high-quality clean tags according to the FastQC (V 0.10.1). Chimeric sequences were filtered using VerSeach software (v2.3.4). Sequences with  $\geq 97\%$  similarity were assigned to the same operational taxonomic units (OTUs) by VerSeach (v2.3.4). Representative sequences were chosen for each OTU, and taxonomic data were then assigned to each representative sequence using the ribosomal database project classifier. The differences of the dominant species in different groups and multiple sequence alignment were conducted using PyNAST software to study phylogenetic relationship of different OTUs. Abundance information of OTUs was normalized using a standard of a sequence number corresponding to the sample with the least sequences. Alpha diversity is applied in analyzing complexity of species diversity for a sample through 4 indices, including Chao1, Shannon, Simpson, and Observed species. All indices of samples were calculated with QIIME (Version 1.8.0). Beta diversity analysis was used to evaluate differences of samples in species complexity. Beta diversity was calculated by principle co-ordinates analysis (PCoA) and cluster analysis by QIIME software (Version 1.8.0). The Spearman's rho nonparametric correlations between the gut microbiota and health-related indexes were determined using R packages (V2.15.3).

Alpha diversity indexes, relative abundance of phyla, principal component analysis, and linear discriminant analysis (LDA) effect size (LEFse) analysis were assessed.

**2.8. Cecal and Colonic Short-Chain Fatty Acids.** Production of SCFA in the ceca and feces of mice was analyzed using a 7890A GC (Agilent Technologies, Stockport, UK) using a slightly modified method.<sup>6</sup> Detailed description of these methods is described in a previous study.

**2.9. Statistical Analysis.** Data were expressed as means  $\pm$  SD. Statistical analysis was performed using GraphPad Prism V.7.04 (GraphPad Software, USA). One-way analysis of variance (ANOVA) for multiple comparisons was conducted, followed by the non-

parametric Kruskal–Wallis test with Dunnett's multiple comparisons test.<sup>37</sup> Significance was set at  $p < 0.05$ .

### 3. RESULTS

**3.1. WRP Prevented Body Weight Gain in HFD-Induced Obese Mice.** To test the effects of pectin supplementation on body weight, we fed mice with HFD with or without pectin supplementation for 8 weeks. Compared with the CD, mice fed with an HFD showed a significant and sustained increase body weight (260%) (Figure 1). Notably, WRP supplementation dramatically prevented the body weight gain caused by HFD ( $p < 0.001$ , Figure 1B,C). However, no significant improvement in weight gain was observed in HFD-CP and HFD-DWRP groups. As shown in Figure 1C–E, HFD significantly induced the weight gain of liver, kidney, iWAT, and epididymal white adipose tissue of mice. In parallel with weight gain caused by HFD (Figure 1E), the weight gain of white adipose tissue and visceral fat of HFD fed mice was prevented to decrease observably when intervened by WRP (iWAT,  $p < 0.001$ ; eWAT,  $p < 0.01$ ). Besides, WRP apparently reduced macrosteatosis and hepatocyte ballooning in the livers of obese mice. The liver and fat tissue morphology in HFD-CP and HFD-DWRP groups was the same as in the HFD. The fat tissue morphology was not maintained in HFD-CP and HFD-DWRP groups (Figure 2).

Some reports suggested that fucoidan was reported to affect appetite regulation and subsequent control of body weight.<sup>38</sup> There was no significant difference in food intake between groups (see Figure S1), indicating that the mitigating effects of WRP on HFD-induced obesity in mice were not through reduced food consumption.

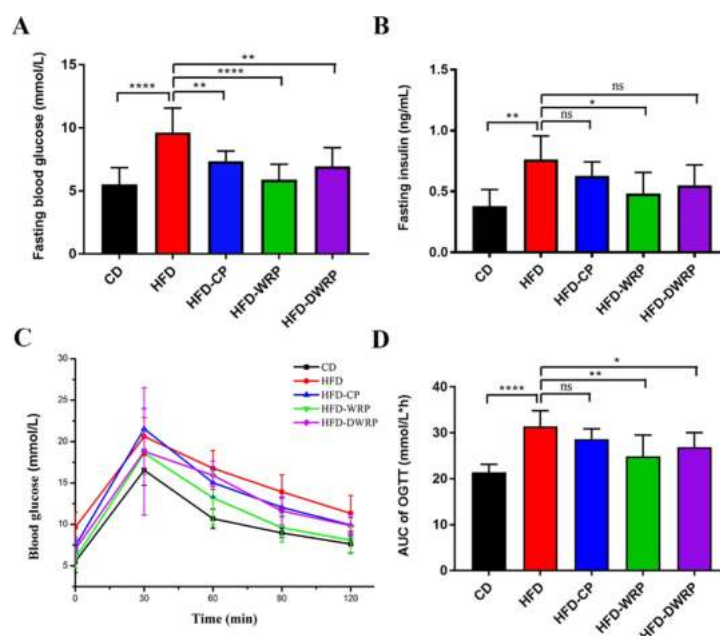


**Figure 3.** Effects of CP, WRP, and DWRP on the development of insulin resistance in HFD-fed mice. (A) Fasting blood glucose; (B) fasting insulin; (C) blood glucose; and (D) AUC of OGTT are shown. (\* $p < 0.05$ ; \*\* $p < 0.01$ ; \*\*\* $p < 0.001$ ; and \*\*\*\* $p < 0.0001$ ; ns, not significant.).

**3.2. WRP Alleviated HFD-Induced Hyperlipidemia, Hyperglycemia, and Inflammatory Responses.** As shown in Table 1, the serum level of total triacylglycerol (TG), TC, LDL-C, and free fatty acids (FFAs) in mice were negatively controlled and the (HDL-C), adiponectin, and HDL-C/LDL-C content were positively controlled by WRP treatment.<sup>39</sup> Pro-inflammatory cytokines have been shown systemic inflammation but also insulin resistance,<sup>40</sup> and bacterial LPS is an early factor in the triggering of metabolic diseases induced by obesity.<sup>41</sup> The adipose tissues of obese animals and humans secreted considerable levels of pro-inflammatory cytokines and LPS compared with lean individuals.<sup>40,42</sup> In the present study, supplementation of WRP and DWRP significantly controlled the level of serum LPS and TNF- $\alpha$  in HFD-fed mice. Further, to determine the effect of different pectins on glucose homeostasis and insulin sensitivity, OGTT and fasting insulin test were performed. As shown in Figure 3, HFD treatment impeded the glucose utilization ability as the levels of fasting blood glucose ( $p < 0.0001$ ) and insulin ( $p < 0.01$ ) were significantly increased compared to the CD group. Nevertheless, WRP-intervened HFD-fed mice exhibited lower glucose levels at all time points up to 120 min after oral glucose challenge and reduced AUC glycemic response. Moreover, WRP and DWRP supplementation lowered the plasma levels of glucose and insulin compared with the HFD group (Figure 3D). Together, WRP effectively alleviated the dyslipidemia induced by HFD through negative control of blood lipid and proinflammatory factor content; on the other hand, WRP improved the glucose intolerance and insulin sensitivity.

**3.3. WRP Promotes Browning of White Adipocytes in HFD-Induced Mice.** The average cell size of iWAT in the HFD group was significantly larger than the CD group (Figure 4A). WRP supplementation of the size of iWAT is significantly lower than the HFD group, but no obvious difference in size of

iWAT was observed in both HFD-CP and HFD-DWRP groups. Under some stimulation (cold condition or  $\beta$ -3 adrenergic agonist), the content of mitochondria in WATs increased dramatically and enhanced thermogenic properties. This process was called “browning”, and brown-like adipocytes expressed large amounts of UCP1 to enhance energy expenditure in WATs.<sup>43</sup> As expected, the immunohistochemistry staining results revealed that the expression level of UCP1 protein in iWAT was remarkably upregulated in the HFD-WRP group compared to the HFD group (Figure 4A). Consistent with these changes, qPCR analysis confirmed that WRP increased the mRNA level of UCP1 in iWAT (5.65-fold vs HFD group,  $p < 0.001$ ) (Figure 4B). In addition, supplementation of WRP also remarkably increased the expression of some thermogenic genes and beige adipocyte-selective markers in iWAT, such as PRDM16 ( $p < 0.0001$ ), PGC-1 $\alpha$  ( $p < 0.01$ ), ERR $\alpha$  ( $p < 0.05$ ), mtTFA ( $p < 0.05$ ), Tmem26 ( $p < 0.05$ ), CD137 ( $p < 0.01$ ), and Cidea ( $p < 0.01$ ) (Figure 4B,C). These findings demonstrated that supplementation of WRP stimulates browning of iWAT and increased adaptive thermogenesis in HFD-fed mice.

**3.4. WRP Prevents HFD-Induced Gut Dysbiosis in Mice.** Sequencing analysis of caecal samples from WRP-intervened mice produced an average of  $1179 \pm 156$  observed species compared to the HFD group ( $960 \pm 51$ ) (see Table S3). Next,  $\alpha$ -diversity analysis was performed to determine the community richness and diversity. Significant differences in the richness (Chao estimator) and diversity index (Shannon and Simpson index) were detected with the HFD and HFD-WRP groups. In addition, both CP and DWRP showed no remarkable effect on the gut microbiota richness. WRP mitigated the phenomenon of extremely reduced gut microbiota species richness and diversity caused by HFD (see Table S3). The  $\beta$ -diversity analysis based on PCoA plots of weighted UniFrac distance and UPGMA showed that significant

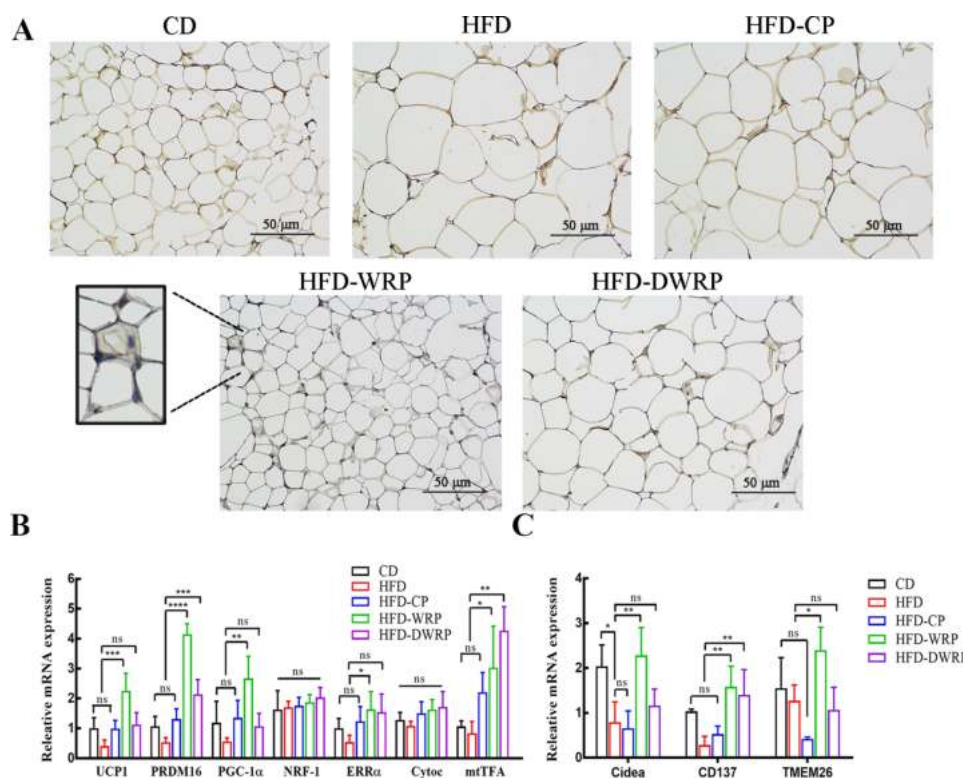


**Figure 4.** RG-I enriched pectin promoted thermogenesis and browning in iWAT of HFD-fed C57BL/6J mice. (A) Immunohistochemistry for UCP1 protein in iWAT of HFD-fed C57BL/6J mice (magnification 200 times). (B) Thermogenic genes and (C) beige adipocyte-selective markers in iWAT. Relative mRNA expression of UCP1, PRDM16, PGC-1 $\alpha$ , nuclear respiratory factor-1, estrogen-related receptor  $\alpha$ , cytochrome *c* (Cytoc), mitochondrial transcription factor A (mtTFA), Cidea, CD137, and TMEM26 was assessed by qRT-PCR and was compared to the HFD group. Results are expressed as mean  $\pm$  SD ( $n \geq 5$ ). ns, not significant. (\*) (\*\*) (\*\*\*)  $p < 0.05, 0.01, 0.001$ , compared to the HFD group based on ANOVA with Duncan's range tests.

separation was observed between HFD-WRP and HFD groups, and there was also a clear dividing line among the CD, HFD, and HFD-WRP groups (Figure 5A,B). Collectively, these results indicated that WRP intensively alleviates the gut microbiota dysbiosis in HFD-fed mice compared to CP and DWRP.

At the phylum level (Figure 5C), HFD markedly increased the Firmicutes/Bacteroidetes (F/B) ratio to 8.78 compared to 1.44 in the CD group. WRP supplementation reduced F/B ratio to 1.72 in obese mice which is comparable to that of the CD group, while HFD-CP and HFD-DWRP groups were with a ratio of 8.52 and 6.30 respectively (Figure 5C, Table S4). The relative abundance of Proteobacteria in HFD-fed mice was significantly higher. Nevertheless, the Proteobacteria level showed an inconspicuous decline under the intervention of CP, WRP, and DWRP. At the class level (Figure 5D), the Bacteroidia (Bacteroidetes phylum) comprised  $36.27 \pm 14.43$ ,  $15.72 \pm 12.05$ ,  $8.83 \pm 4.73$ ,  $23.49 \pm 5.41$ , and  $12.16 \pm 7.12\%$  of gut microbiota in CD, HFD, HFD-CP, HFD-WRP, and HFD-DWRP groups. WRP significantly enhanced the abundance of Bacteroidia in the caecum of HFD-fed mice ( $p < 0.05$ , see Table S4). In contrast, WRP reversed the increase tendency on the abundance of Clostridia (Firmicutes phylum) caused by HFD. Additionally, predominant bacteria in the caecum of mice were Lachnospiraceae (Firmicutes phylum) and Porphyromonadaceae (Bacteroidetes phylum) at the

family level (see Figure S2). As shown in Table S4, the relative abundance of Lachnospiraceae in CD, HFD, and HFD-WRP group were  $40.38 \pm 7.23$ ,  $61.98 \pm 8.26$ , and  $46.42 \pm 7.85\%$ , respectively. On the other side, the relative abundance of Porphyromonadaceae in CD, HFD, and HFD-WRP groups were  $23.80 \pm 4.64$ ,  $4.14 \pm 1.43$ , and  $15.92 \pm 6.78\%$ . The results based on the class and family level also explained the decrease of F/B ratio with WRP supplementation. At the genus level, Un-Lachnospiraceae and Acetatifactor were predominant bacteria (average relative abundance above 10%), the rest consisted of *Lachnoclostridium*, *Acetatifactor*, *Olsenella*, *Lactobacillus*, *Butyrivibrio*, *Alistipes*, *Desulfovibrio*, and *Bacteroides* with an average relative abundance below 5% (Figure 5E). HFD feeding significantly increased the obesity-related bacteria in the caecum of mice, such as *Acetatifactor* and *Olsenella*, while WRP significantly declined the relative abundance of these bacteria (Figure 4E, Table S4). In addition, the obesity negative-related bacteria (*Barnesiella* and *Butyrivibrio*) were enriched under the intervention of WRP.

Figure 6 shows that pathogenic taxa Firmicutes, Clostridia, Clostridiales, Lachnospiraceae, *Acetatifactor*, and *Desulfovibrio* were higher in the HFD group compared to the CD group, while the beneficial phylotypes Bacteroidetes, *Bifidobacterium*, *Butyrivibrio*, Porphyromonadaceae, *Alloprevotella*, *Anaerostipes*, and *Anaerotaenia* were enriched in the CD group. After

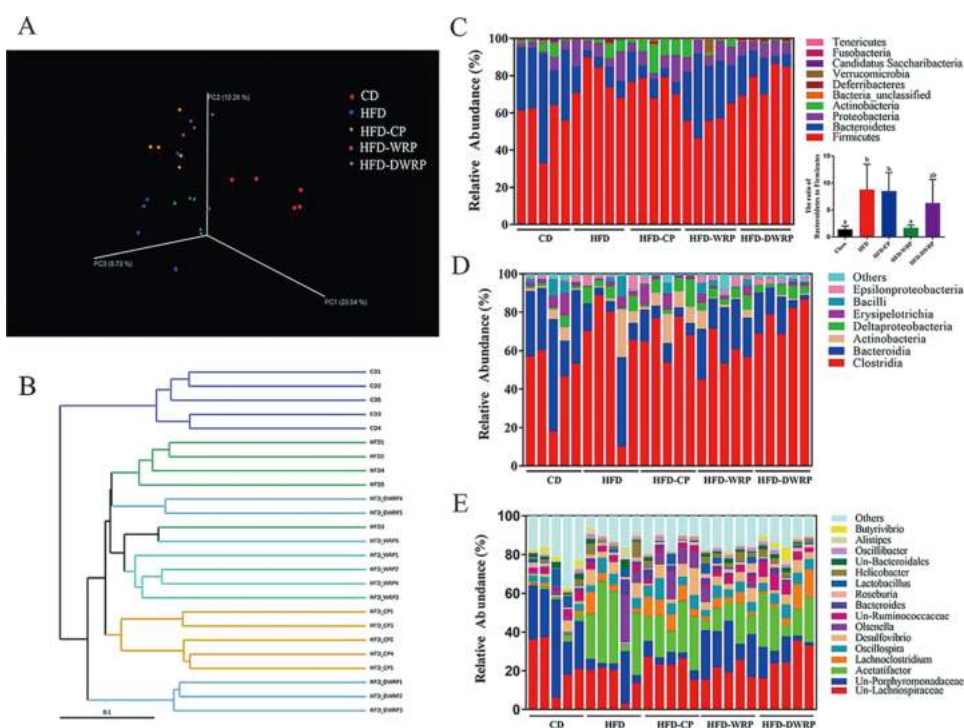


**Figure 5.** Structural composition of gut microbiota. (A) PCoA plot of cecal microbiota in HFD-fed mice based on weighted UniFrac metric. (B) UPGMA analysis of cecal microbiota of HFD-fed mice. Cecal microbiota in CD, HFD, HFD-CP, HFD-WRP, and HFD-DWRP groups at phylum (C), class (D), and genus (E) levels.

treating with CP, there were only two significant different OUT units. Notably, 19 remarked different OUT units were observed in the HFD-WRP group (LDA score threshold > 3 were listed). Figure 6C presented the dominate bacteria taxon in the caecum of HFD-fed mice intervened by WRP. Specifically, WRP supplementation significantly increased the abundance of Bacteroidia, Bacteroidales, Barnesiella, Butyrivibrio, Roseburia, Prophymonadaceae, Flavonifractor, Acetivibrio, and Clostridium cluster IV, while HFD-DWRP group enriched the obesity-related Butyrivibrio and Mucispirillum genus. The gut dysbiosis induced by HFD was effectively modulated after treatment of WRP, which was due to the more complex RG-I domain stimulating the growth of intestinal microorganisms.

**3.5. WRP Treatment Promotes Generation of SCFAs in HFD-Induce Mice.** The gut microbiota was modulated by WRP supplementations in HFD-fed mice; thus, we investigated the effect of WRP on SCFAs-microbial metabolites.<sup>44</sup> HFD significantly inhibited total SCFAs, acetate, and propionate in obese mice caecum but had no effect on butyrate generation (Figure 7). CP, WRP, and DWRP treatments remarkably prevented the suppression of caecal total SCFAs, acetate, and valerate. The fermentation of galacturonic acid and xylose were reported to promote the production of acetate and butyrate, while the production of propionate were promoted by arabinose and glucose fermentation.<sup>45</sup> The increase production of propionate in HFD-WRP and HFD-DWRP may be due to the higher content of arabinose and rhamnose in RG-I pectin compared to CP.<sup>23</sup> Compared with CD group, HFD significantly decreased the acetate, butyrate, and valerate levels in the

colon feces except propionate. Notably, only the HFD-WRP group contained significantly higher concentrations of all kinds of SCFAs in obese mice colon compared to the HFD group. However, no significant improvement of these SCFAs was observed in both HFD-CP and HFD-DWRP groups.

**3.6. Correlation of Gut Microbiota with Obesity-Related Indexes.** The Spearman's correlation analysis was performed to clarify the correlation among the microbiota and obesity-related indexes (Figure 8). *Pseudoflavonifractor*, *Desulfovibrionaceae*, *Acetatifactor*, *Lachnospirillum*, and *Robinsoniella* were strongly positively correlated with body weight, epididymal fat weight, TG, TC, and insulin, whereas they were strongly negatively correlated with the gut tissue index ( $p < 0.01$  or  $p < 0.05$ ), suggesting that they may be the most significant genera for the development of obesity. In addition, the Simpson index, Bifidobacterium, Propionomonadaceae, *Acetanaerobacterium*, *Alloprevotella*, *Prevotella*, *Acetivibrio*, *Acetatifactor*, *Prevotella*, *Gemella*, *Eubacterium*, *Ruminococcus*, *Butyrivibrio*, and *Clostridium\_sensu\_stricto* were highly positively correlated with the gut tissue index, while they were highly negatively correlated with body weight, epididymal fat weight, TG, total cholesterol, and LPS ( $p < 0.01$  or  $p < 0.05$ ), indicating that they may play the most important role in the obesity.

## 4. DISCUSSION

**4.1. RG-I Content, Molecular Weight, and Branching Chains are Key Factors of Pectin to Prevent Obesity.** In our previous research, we found that WRP and DWRP had a positive modulation of gut prebiotic microbiota, which stimulated our interests in the potential anti-obesogenic effects

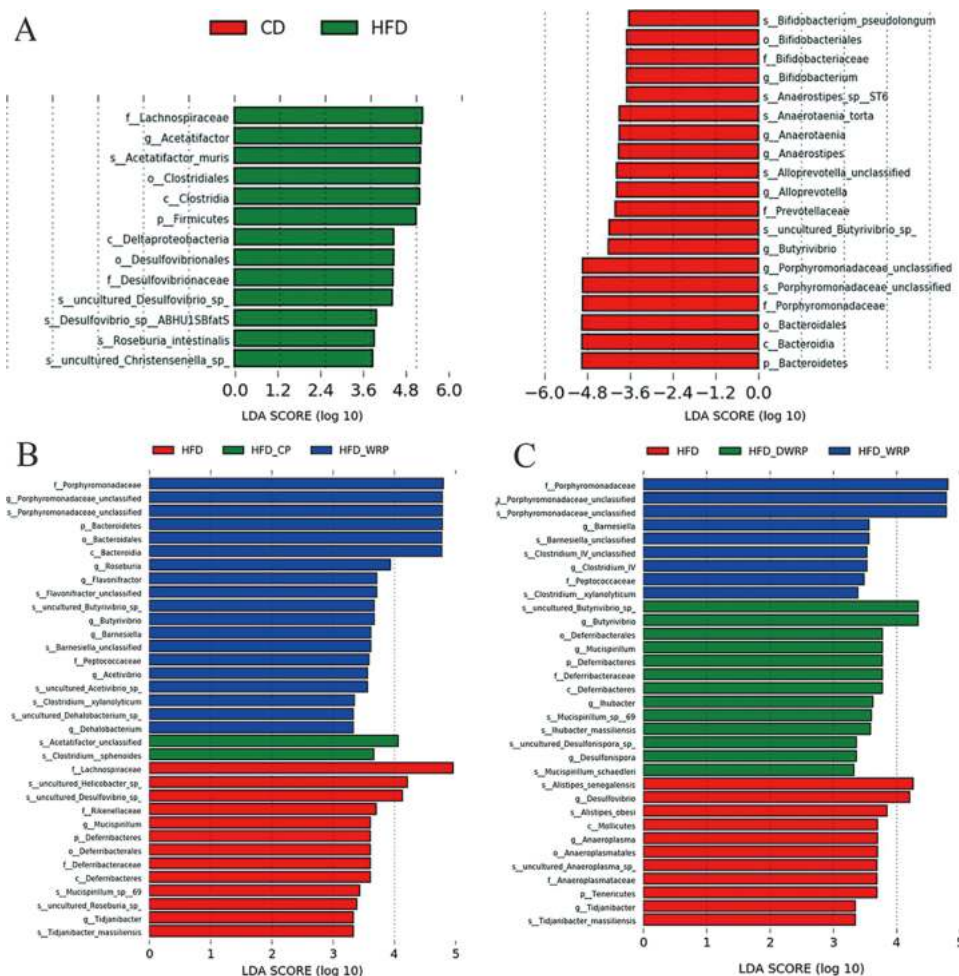


**Figure 6.** LefSe comparison of gut microbiota. (A) LDA score between CD and HFD groups, with LDA score  $> \pm 3.6$ ; (B) LDA score between CD, HFD-WRP, and HFD-CP groups, with LDA score  $> 3.3$ ; (C) LDA score between CD, HFD-WRP, and HFD-DWRP groups, with LDA score  $> 3.3$ .

of RG-I enriched pectin and its oligosaccharides.<sup>32,35</sup> However, the gut microbiota of mice changed dramatically under the condition of HFD feeding, and in turn, they might affect the ferment of pectin in the microbiota. In the present study, we first found that WRP with a high molecular size (531.5 kDa) and RG-I content (70.44%) mitigated against the HFD-induced body weight gain, adipocyte hypertrophy, fatty liver, and hyperlipidemia without suppressing the food intake. On the contrary, no significant decrease in body weight gain was discovered after oral administration of CP (rich in HG domain) and DWRP (depolymerized from WRP). This indicates that the content and molecular structure of RG-I enriched pectin are important for its biological function. Bacterial species characteristic of lean hosts, such as *Butyrivibrio*, *Roseburia*, *Prophylomonadaceae*, *Barnesiella*, *Flavonifractor*, *Acetivibrio*, and *Clostridium* cluster IV, were largely enriched in HFD-WRP group. The anti-obesogenic effects would be explained by the production of SCFAs which could regulate energy homeostasis. Meanwhile, CP and DWRP supplementation barely motivated the enrichment of beneficial bacteria or the diversity of gut microbiota in obese mice.

Notably, data published by our group exactly had shown convincingly that CP intervention has no potential beneficial effect on the gut microbiota of the chow diet feeding mice.<sup>32</sup> We tentatively linked the reason to easy accessibility of the pectic backbone (due to less RG-I branches) to microbial degrading enzymes and single monosaccharide composition, which activated much less microbiota species into the fermentation of CP. Multiple species from Bacteroidetes phylum harbored very broad potential to utilize the RG-I domain from pectin.<sup>22</sup> As described by Li et al., RG-I pectin purified from *Fructus Mori* promoted the growth of *Bacteroides thetaiotaomicron*, a dominant gut bacteria strain shown to be beneficial for the intestinal mucosa of human.<sup>46</sup> The intricate RG-I pectin comprised complex side-chain components (arabinan, galactan, and arabinogalactan) contributed significantly to the gut microbiota fermentation and favorable changes in microbiota composition.<sup>21,31</sup> Therefore, the high RG-I domain content contributed significantly to the capacity of pectin in HFD-induced obesity modulation.

As highlighted by others, pectic oligosaccharides better promoted growth of beneficial bacteria and had the potential to reduce metabolic conditions such as obesity.<sup>11,30,47</sup> In here,



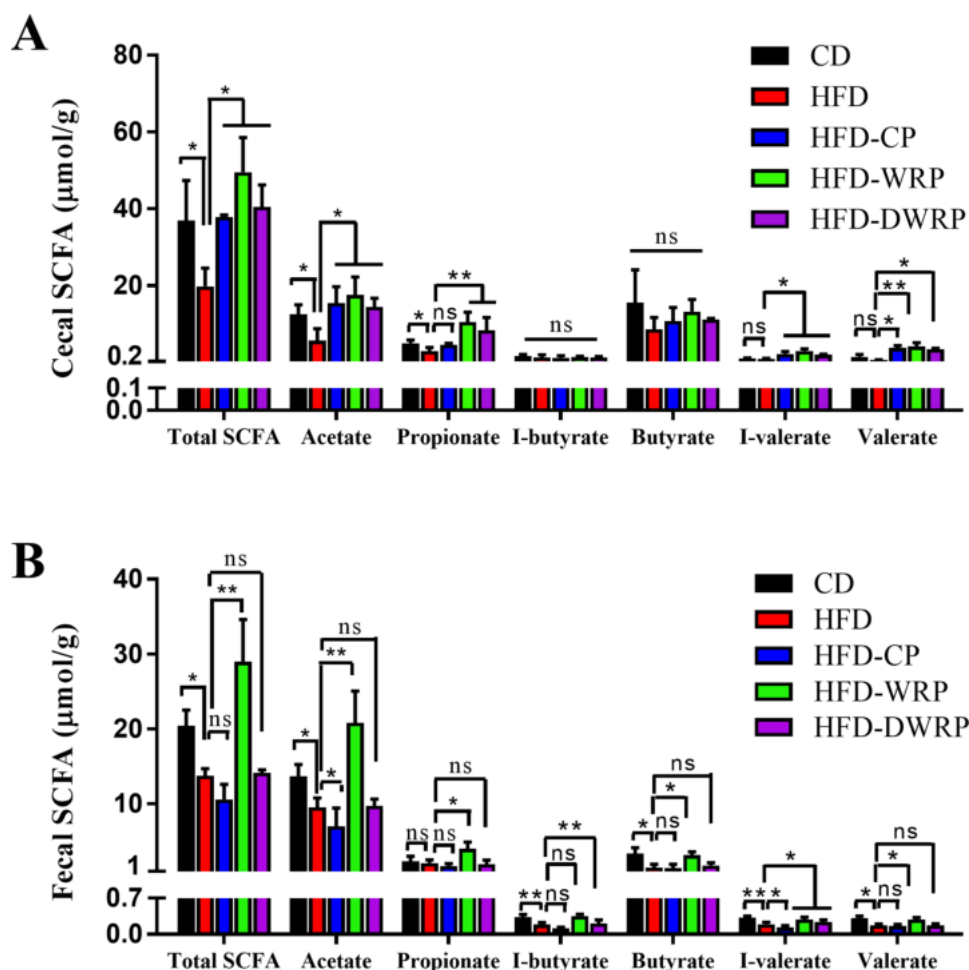


**Figure 7.** Concentration ( $\mu\text{mol/g}$ ) of acetic, propionate, butyrate, I-butyrate, valerate, and I-valerate in the cecal contents (A) and colon feces (B) of the pectin-treated group and the chow diet group.

WRP supplementation mitigated the gut microbiota of HFD-fed mice dramatically. Paradoxically, no modulation effect of gut microbiota was observed in the HFD-DWRP group (Figure 6). Specifically, many reports have confirmed that a greater proportion of Ara and Gal in RG-I pectin promoted the growth of *Bacteroides* species.<sup>31–33</sup> Compared to WRP [Rha/(Gal + Ara) ratio of around 1:20], DWRP [Rha/(Gal + Ara) = 1:6] had much less degree of Ara and Gal side chains; so large  $M_w$  WRP might better regulate the gut microbiota of obese mice.<sup>48</sup> It is also worth noting that the fermentation effect of DWRP in gut of obese mice may be different from pectic oligosaccharides which is mainly composed of GalA studied in most articles. Concretely, *Barnesiella* and *Clostridium* cluster IV which negatively correlated to obesity were restored in the HFD-WRP group, while the HFD-DWRP group enriched the *Mucispirillum* genus (Figure 6). The increased levels of *Mucispirillum* was closely correlated with obesity, which suggested that no anti-obesity effect was observed in the HFD-DWRP group may due to *Mucispirillum*-induced gut dysbiosis.<sup>49</sup> This could also give a clue as to why DWRP could not inhibit the HFD-induced body weight gain: the low branching degree structural RG-I domain and low  $M_w$  of

DWRP led a halfway rectification of gut dysbiosis in obese mice.

Our results showed that highly branched RG-I enriched pectin with large molecular size is a strong candidate in prevention of HFD-induced obesity.

**4.2. WRP Alleviates the HFD-Induced Obesity via Regulation of Gut Dysbiosis and Adipocytes Thermogenesis.** In this study, HFD caused an increase in the Firmicutes/Bacteroidetes ratio (F/B), which was reported to be related to obesity,<sup>50</sup> whereas WRP supplementation reduced the F/B ratio remarkably (Table 1, Figure 5) because the capacity to utilize RG-I was widespread among colonic Bacteroidetes but relatively uncommon among Firmicutes.<sup>23</sup> Furthermore, we observed that changes in the level of Lachnospiraceae, *Acetatifactor*, *Desulfovibrio*, *Olsenella*, *Alistipes*, and *Mucispirillum* were higher in the HFD group. Bacteroidales, *Butyrivibrio*, *Roseburia*, *Prophyromonadaceae*, *Barnesiella*, *Flavonifractor*, *Acetivibrio*, and *Clostridium* cluster IV were restored with WRP supplementation. With regard to the Firmicutes phylum, HFD produced an increase in Lachnospiraceae, which is a potent Firmicutes family related to the regulation of immune and obesity.<sup>51</sup> Here, we observed that changes in the level of Lachnospiraceae were significantly higher



with an increased abundance of *Olsenella* in pectin or fructo-oligosaccharides-fed mice.<sup>61,62</sup> However, as highlighted by some researchers, *Olsenella* could be a target bacterial flora for obesity because it was enriched considerably in HFD-fed mice.<sup>52,63,64</sup> Based on our findings, the abundance of *Olsenella* was enriched by HFD, while it reduced to the level close to the CD group after WRP supplementation. Our results exhibit a high level of *Acetivibrio* in the HFD-WRP group and negatively correlated with body weight ( $p < 0.01$ ), TC ( $p < 0.05$ ). Data published by Yang et al. showed that maize-derived feruloylated polysaccharides significantly increased *Acetivibrio* and controlled the weight gain induced by HFD.<sup>65</sup> One hypothesis is that multiple GH secreted from the *Acetivibrio* hydrolyzed arabinose side chain of WRP and stimulated SCFA production, as the cecal butyrate level positively correlated with *Acetivibrio*.<sup>66</sup>

A previous research has illustrated that HFD triggered inflammatory responses, defecting gut barrier integrity and increasing the cytokines.<sup>59</sup> In our model, WRP treatment significantly decreased the levels of serum LPS and TNF- $\alpha$  in HFD-fed mice. Specifically, the LPS-producing microbiota such as *Desulfovibrio* and *Mucispirillum* became abundant after HFD feeding.<sup>52</sup> Notably, *Mucispirillum* has been described as a mucus-associated bacterium that bursts during inflammation in the HFD-induced obese mouse model.<sup>67</sup> *Desulfovibrio* is one kind of genus belonging to Desulfovibrionaceae and Proteobacteria, positively related to obesity-induced inflammation.<sup>68</sup> Moreover, the correlation analysis further verified the significant correlation between *Desulfovibrio* and these obesity-related indexes (Figure 8).

On the other hand, butyrate and other short chain fatty acids are known to inhibit fat accumulation and adipocyte dysfunction.<sup>69</sup> Here, we found that WRP intervention significantly enriched the fecal and cecal butyrate. Moreover, the correlation analysis verified the positive association of microbiota diversity with cecal butyrate. Several studies reported that *Barnesiella*, *Roseburia*, *Clostridium* cluster IV, and *Butyrivibrio* are highly associated with the production of SCFAs, especially the synthesis of butyrate.<sup>49</sup> Moreover, suppression of HFD-induced body weight gain of WRP could be related to SCFAs secreted by relevant microbes (Figure S2). In line with this, it has been revealed that WRP treatment enriched these microbes and prevented the HFD-induced gut dysbiosis in mice.

Interestingly, a crucial analysis revealed that SCFAs can stimulate the white adipose tissue browning.<sup>70</sup> Consistently, we also found that WRP supplementation reduced the white adipose tissue's weight and upregulated UCP1 expression, a specific protein uncoupling respiration from ATP synthesis and generating heat (Figure 4). Moreover, WRP showed potential in fat browning by activating PGC-1 $\alpha$ , a master regulator of mitochondrial biogenesis.<sup>71</sup> Compared with the HFD group, gene expressions of the beige adipocyte-selective markers including UCP1, TMEM26, CD137, and Cidea were markedly increased in the HFD-WRP group (Figure 4B,C). The above results indicated that the supplementation of WRP triggered the browning of iWAT in HFD-fed mice.

Overall, we found that WRP can attenuate HFD-induced obesity, inflammation, and gut dysbiosis through combined effects of the white adipose browning and gut microbiota modulation, while the CP (HG dominated pectin) and DWRP (less branched RG-I oligosaccharide) have only limited effects on resistance to HFD-induced obesity. Our findings convinced

that highly branched RG-I domain enrichment is essential for pectin mitigating against the HFD-induced obesity.

## ■ ASSOCIATED CONTENT

### Supporting Information

The Supporting Information is available free of charge at <https://pubs.acs.org/doi/10.1021/acs.jafc.0c02654>.

Compositions and energy densities of the diets; specific formula of the HFD; diversity and richness of cecal microbiota in CP, WRP, and DWRP supplements altering the diversity; abundance of key phylogenotypes of gut microbiota in HFD-fed C57BL/6J mice; PCR primers used in this study; weekly food intake (A) and average food intake (B) of mice in response to dietary CP, WRP, and DWRP; and LEfSe comparison of cecal microbiota (PDF)

## ■ AUTHOR INFORMATION

### Corresponding Author

**Shiguo Chen** – College of Biosystems Engineering and Food Science, National-Local Joint Engineering Laboratory of Intelligent Food Technology and Equipment, Zhejiang Key Laboratory for Agro-Food Processing Integrated Research Base of Southern Fruit and Vegetable Preservation Technology, Zhejiang International Scientific and Technological Cooperation Base of Health Food Manufacturing and Quality Control, Fuli Institute of Food Science, and Ningbo Research Institute, Zhejiang University, Hangzhou 310058, China; [orcid.org/0000-0002-6439-7735](https://orcid.org/0000-0002-6439-7735); Email: [chenshiguo210@163.com](mailto:chenshiguo210@163.com)

### Authors

**Kai Zhu** – College of Biosystems Engineering and Food Science, National-Local Joint Engineering Laboratory of Intelligent Food Technology and Equipment, Zhejiang Key Laboratory for Agro-Food Processing Integrated Research Base of Southern Fruit and Vegetable Preservation Technology, Zhejiang International Scientific and Technological Cooperation Base of Health Food Manufacturing and Quality Control, Zhejiang University, Hangzhou 310058, China

**Guizhu Mao** – College of Biosystems Engineering and Food Science, National-Local Joint Engineering Laboratory of Intelligent Food Technology and Equipment, Zhejiang Key Laboratory for Agro-Food Processing Integrated Research Base of Southern Fruit and Vegetable Preservation Technology, Zhejiang International Scientific and Technological Cooperation Base of Health Food Manufacturing and Quality Control, Zhejiang University, Hangzhou 310058, China

**Dongmei Wu** – College of Biosystems Engineering and Food Science, National-Local Joint Engineering Laboratory of Intelligent Food Technology and Equipment, Zhejiang Key Laboratory for Agro-Food Processing Integrated Research Base of Southern Fruit and Vegetable Preservation Technology, Zhejiang International Scientific and Technological Cooperation Base of Health Food Manufacturing and Quality Control, Zhejiang University, Hangzhou 310058, China

**Chengxiao Yu** – College of Biosystems Engineering and Food Science, National-Local Joint Engineering Laboratory of Intelligent Food Technology and Equipment, Zhejiang Key Laboratory for Agro-Food Processing Integrated Research Base of Southern Fruit and Vegetable Preservation Technology, Zhejiang International Scientific and Technological Cooperation

Base of Health Food Manufacturing and Quality Control, Zhejiang University, Hangzhou 310058, China

**Huan Cheng** – College of Biosystems Engineering and Food Science, National-Local Joint Engineering Laboratory of Intelligent Food Technology and Equipment, Zhejiang Key Laboratory for Agro-Food Processing Integrated Research Base of Southern Fruit and Vegetable Preservation Technology, Zhejiang International Scientific and Technological Cooperation Base of Health Food Manufacturing and Quality Control, Fuli Institute of Food Science, and Ningbo Research Institute, Zhejiang University, Hangzhou 310058, China

**Hang Xiao** – College of Biosystems Engineering and Food Science, National-Local Joint Engineering Laboratory of Intelligent Food Technology and Equipment, Zhejiang Key Laboratory for Agro-Food Processing Integrated Research Base of Southern Fruit and Vegetable Preservation Technology, Zhejiang International Scientific and Technological Cooperation Base of Health Food Manufacturing and Quality Control, Zhejiang University, Hangzhou 310058, China; Department of Food Science, University of Massachusetts, Amherst, Massachusetts 01003, United States

**Xingqian Ye** – College of Biosystems Engineering and Food Science, National-Local Joint Engineering Laboratory of Intelligent Food Technology and Equipment, Zhejiang Key Laboratory for Agro-Food Processing Integrated Research Base of Southern Fruit and Vegetable Preservation Technology, Zhejiang International Scientific and Technological Cooperation Base of Health Food Manufacturing and Quality Control, Fuli Institute of Food Science, and Ningbo Research Institute, Zhejiang University, Hangzhou 310058, China

**Robert J. Linhardt** – Center for Biotechnology and Interdisciplinary Studies, Rensselaer Polytechnic Institute, Troy, New York 12180, United States; [orcid.org/0000-0003-2219-5833](https://orcid.org/0000-0003-2219-5833)

**Caroline Orfila** – School of Food Science and Nutrition, University of Leeds, Leeds LS2 9JT, U.K.; [orcid.org/0000-0003-2564-8068](https://orcid.org/0000-0003-2564-8068)

Complete contact information is available at: <https://pubs.acs.org/10.1021/acs.jafc.0c02654>

#### Author Contributions

S.C. conceived the study; K.Z. wrote the manuscript; G.M. designed experiments, performed the animal studies and statistical analysis; D.W. contributed to sample preparation; C.Y. helped to perform the animal studies; H.X. helped to revise the manuscript; X.Y., R.J.L. and C.O. interpreted the data; S.C. critically revised the manuscript. All authors read and approved the final manuscript.

#### Funding

This work was financially supported in part by National Key R&D Program of China (2017YFE0122300), National Natural Science Foundation of China (3187181559) and Key R&D Program of Zhejiang Province (2020C02033) and 18CXZ044.

#### Notes

The authors declare no competing financial interest. The animal study was reviewed and approved by Zhejiang Chinese Medicine University IACUC-20180917-02.

#### ACKNOWLEDGMENTS

We thank Baokun Xie for his assistant to the graphs editing to this publication.

#### ABBREVIATIONS

BAT, brown adipose tissue; CD, normal chow diet; DWRP, depolymerized fraction of RG-I enriched pectin from citrus segment membrane; HDL, high density lipoprotein; HFD, high fat diet; OTU, operational taxonomic units; OGTT, oral glucose tolerance test; PGC-1 $\alpha$ , peroxisome proliferator-activated receptor- $\gamma$  coactivator 1-alpha; RG-I, rhamnogalacturonan-I; LDL, low density lipoprotein; LefSe, linear discriminant analysis effect size; TG, total triacylglycerol; TC, total cholesterol; TNF- $\alpha$ , tumor necrosis factor- $\alpha$ ; UCP1, uncoupling protein 1; WAT, white adipose tissue; WRP, RG-I enriched pectin from citrus segment membrane

#### REFERENCES

- (1) Tagliabue, A.; Elli, M. The role of gut microbiota in human obesity: Recent findings and future perspectives. *Nutr., Metab. Cardiovasc. Dis.* **2013**, *23*, 160–168.
- (2) Zmora, N.; Suez, J.; Elinav, E. You are what you eat: diet, health and the gut microbiota. *Nat. Rev. Gastroenterol. Hepatol.* **2019**, *16*, 35–56.
- (3) Stephens, R. W.; Arhire, L.; Covasa, M. Gut Microbiota: From Microorganisms to Metabolic Organ Influencing Obesity. *Obesity* **2018**, *26*, 801–809.
- (4) Bäckhed, F.; Ding, H.; Wang, T.; Hooper, L. V.; Koh, G. Y.; Nagy, A.; Semenkovich, C. F.; Gordon, J. I. The gut microbiota as an environmental factor that regulates fat storage. *Proc. Natl. Acad. Sci. U.S.A.* **2004**, *101*, 15718–15723.
- (5) Ridaura, V. K.; Faith, J. J.; Rey, F. E.; Cheng, J.; Duncan, A. E.; Kau, A. L.; Griffin, N. W.; Lombard, V.; Henrissat, B.; Bain, J. R.; Muehlbauer, M. J.; Ilkayeva, O.; Semenkovich, C. F.; Funai, K.; Hayashi, D. K.; Lyle, B. J.; Martini, M. C.; Ursell, L. K.; Clemente, J. C.; Van Treuren, W.; Walters, W. A.; Knight, R.; Newgard, C. B.; Heath, A. C.; Gordon, J. I. Gut Microbiota from Twins Discordant for Obesity Modulate Metabolism in Mice. *Science* **2013**, *341*, 1241214.
- (6) Wu, T.-R.; Lin, C.-S.; Chang, C.-J.; Lin, T.-L.; Martel, J.; Ko, Y.-F.; Ojcius, D. M.; Lu, C.-C.; Young, J. D.; Lai, H.-C. Gut commensal *Parabacteroides goldsteinii* plays a predominant role in the anti-obesity effects of polysaccharides isolated from *Hirsutiella sinensis*. *Gut* **2019**, *68*, 248–262.
- (7) Chang, C. J.; Lin, C. S.; Lu, C. C.; Martel, J.; Ko, Y. F.; Ojcius, D. M.; Tseng, S. F.; Wu, T. R.; Chen, Y. Y.; Young, J. D.; Lai, H. C. *Ganoderma lucidum* reduces obesity in mice by modulating the composition of the gut microbiota. *Nat. Commun.* **2015**, *6*, 7489.
- (8) Liu, Y.; Chen, J.; Tan, Q.; Deng, X.; Tsai, P.-J.; Chen, P.-H.; Ye, M.; Guo, J.; Su, Z. Nondigestible Oligosaccharides with Anti-Obesity Effects. *J. Agric. Food Chem.* **2020**, *68*, 4–16.
- (9) Palou, M.; Sánchez, J.; García-Carrizo, F.; Palou, A.; Picó, C. Pectin supplementation in rats mitigates age-related impairment in insulin and leptin sensitivity independently of reducing food intake. *Mol. Nutr. Food Res.* **2015**, *59*, 2022–2033.
- (10) Hu, H.; Zhang, S.; Liu, F.; Zhang, P.; Muhammad, Z.; Pan, S. Role of the Gut Microbiota and Their Metabolites in Modulating the Cholesterol-Lowering Effects of Citrus Pectin Oligosaccharides in C57BL/6 Mice. *J. Agric. Food Chem.* **2019**, *67*, 11922–11930.
- (11) Tingirikari, J. M. R. Microbiota-accessible pectic poly- and oligosaccharides in gut health. *Food Funct.* **2018**, *9*, 5059–5073.
- (12) Mao, G.; Wu, D.; Wei, C.; Tao, W.; Ye, X.; Linhardt, R. J.; Orfila, C.; Chen, S. Reconsidering conventional and innovative methods for pectin extraction from fruit and vegetable waste: Targeting rhamnogalacturonan I. *Trends Food Sci. Technol.* **2019**, *94*, 65–78.
- (13) Wu, D.; Zheng, J.; Mao, G.; Hu, W.; Ye, X.; Linhardt, R. J.; Chen, S. Rethinking the impact of RG-I mainly from fruits and vegetables on dietary health. *Crit. Rev. Food Sci. Nutr.* **2019**, 1–23.
- (14) Zheng, J.; Chen, J.; Zhang, H.; Wu, D.; Ye, X.; Linhardt, R.; Chen, S. Gelling mechanism of RG-I enriched citrus pectin: Role of

- arabinose side-chains in cation- and acid-induced gelation. *Food Hydrocolloids* **2020**, *101*, 105536.
- (15) Chen, J.; Cheng, H.; Zhi, Z.; Zhang, H. Extraction temperature is a decisive factor for the properties of pectin. *Food Hydrocolloids* **2020**, 106160.
- (16) Bang, S.-J.; Kim, G.; Lim, M. Y.; Song, E.-J.; Jung, D.-H.; Kum, J.-S.; Nam, Y.-D.; Park, C.-S.; Seo, D.-H. The influence of in vitro pectin fermentation on the human fecal microbiome. *AMB Express* **2018**, *8*, 98.
- (17) Karboune, S.; Khodaei, N. Structures, isolation and health-promoting properties of pectic polysaccharides from cell wall-rich food by-products: a source of functional ingredients. *Current Opinion in Food Science* **2016**, *8*, 50–55.
- (18) Patnode, M. L.; Beller, Z. W.; Han, N. D.; Cheng, J.; Peters, S. L.; Terrapon, N.; Henrissat, B.; Le Gall, S.; Saulnier, L.; Hayashi, D. K.; Meynier, A.; Vinoy, S.; Giannone, R. J.; Hettich, R. L.; Gordon, J. I. Interspecies Competition Impacts Targeted Manipulation of Human Gut Bacteria by Fiber-Derived Glycans. *Cell* **2019**, *179*, 59–73.e13.
- (19) Jiang, T.; Gao, X.; Wu, C.; Tian, F.; Lei, Q.; Bi, J.; Xie, B.; Wang, H.; Chen, S.; Wang, X. Apple-Derived Pectin Modulates Gut Microbiota, Improves Gut Barrier Function, and Attenuates Metabolic Endotoxemia in Rats with Diet-Induced Obesity. *Nutrients* **2016**, *8*, 126.
- (20) Licht, T. R.; Hansen, M.; Bergström, A.; Poulsen, M.; Krath, B. N.; Markowski, J.; Dragsted, L. O.; Wilcks, A. Effects of apples and specific apple components on the cecal environment of conventional rats: role of apple pectin. *BMC Microbiol.* **2010**, *10*, 13.
- (21) Luis, A. S.; Briggs, J.; Zhang, X.; Farnell, B.; Ndeh, D.; Labourel, A.; Baslé, A.; Cartmell, A.; Terrapon, N.; Stott, K.; Lowe, E. C.; McLean, R.; Shearer, K.; Schückel, J.; Venditto, I.; Ralet, M.-C.; Henrissat, B.; Martens, E. C.; Mosimann, S. C.; Abbott, D. W.; Gilbert, H. J. Dietary pectic glycans are degraded by coordinated enzyme pathways in human colonic Bacteroides. *Nat. Microbiol.* **2018**, *3*, 210–219.
- (22) Martens, E. C.; Lowe, E. C.; Chiang, H.; Pudlo, N. A.; Wu, M.; McNulty, N. P.; Abbott, D. W.; Henrissat, B.; Gilbert, H. J.; Bolam, D. N.; Gordon, J. I. Recognition and degradation of plant cell wall polysaccharides by two human gut symbionts. *PLoS Biol.* **2011**, *9*, No. e1001221.
- (23) Larsen, N.; Bussolo de Souza, C.; Krych, L.; Barbosa Cahu, T.; Wiese, M.; Kot, W.; Hansen, K. M.; Blennow, A.; Venema, K.; Jespersen, L. Potential of Pectins to Beneficially Modulate the Gut Microbiota Depends on Their Structural Properties. *Front Microbiol* **2019**, *10*, 223.
- (24) Luis, A. S.; Martens, E. C. Interrogating gut bacterial genomes for discovery of novel carbohydrate degrading enzymes. *Curr. Opin. Chem. Biol.* **2018**, *47*, 126–133.
- (25) Khodaei, N.; Fernandez, B.; Fliss, I.; Karboune, S. Digestibility and prebiotic properties of potato rhamnogalacturonan I polysaccharide and its galactose-rich oligosaccharides/oligomers. *Carbohydr. Polym.* **2016**, *136*, 1074–1084.
- (26) Bianchi, F.; Larsen, N.; de Mello Tieghi, T.; Adorno, M. A. T.; Kot, W.; Saad, S. M. I.; Jespersen, L.; Sivieri, K. Modulation of gut microbiota from obese individuals by in vitro fermentation of citrus pectin in combination with *Bifidobacterium longum* BB-46. *Appl. Microbiol. Biotechnol.* **2018**, *102*, 8827–8840.
- (27) Shinohara, K.; Ohashi, Y.; Kawasumi, K.; Terada, A.; Fujisawa, T. Effect of apple intake on fecal microbiota and metabolites in humans. *Anaerobe* **2010**, *16*, 510–515.
- (28) Gullón, B.; Gómez, B.; Martínez-Sabajanes, M.; Yáñez, R.; Parajó, J. C.; Alonso, J. L. Pectic oligosaccharides: Manufacture and functional properties. *Trends Food Sci. Technol.* **2013**, *30*, 153–161.
- (29) Gómez, B.; Gullón, B.; Yáñez, R.; Schols, H.; Alonso, J. L. Prebiotic potential of pectins and pectic oligosaccharides derived from lemon peel wastes and sugar beet pulp: A comparative evaluation. *J. Funct. Foods* **2016**, *20*, 108–121.
- (30) Chen, J.; Liang, R.-h.; Liu, W.; Li, T.; Liu, C.-m.; Wu, S.-s.; Wang, Z.-j. Pectic-oligosaccharides prepared by dynamic high-pressure microfluidization and their in vitro fermentation properties. *Carbohydr. Polym.* **2013**, *91*, 175–182.
- (31) Centanni, M.; Carnachan, S. M.; Bell, T. J.; Daines, A. M.; Hinkley, S. F. R.; Tannock, G. W.; Sims, I. M. Utilization of Complex Pectic Polysaccharides from New Zealand Plants (*Tetragonia tetragonioides* and *Corynocarpus laevigatus*) by Gut Bacteroides Species. *J. Agric. Food Chem.* **2019**, *67*, 7755–7764.
- (32) Mao, G.; Li, S.; Orfila, C.; Shen, X.; Zhou, S.; Linhardt, R. J.; Ye, X.; Chen, S. Depolymerized RG-I-enriched pectin from citrus segment membranes modulates gut microbiota, increases SCFA production, and promotes the growth of *Bifidobacterium* spp., *Lactobacillus* spp. and *Faecalibaculum* spp. *Food Funct.* **2019**, *10*, 7828–7843.
- (33) Liu, Y.; Heath, A.-L.; Galland, B.; Rehrer, N.; Drummond, L.; Wu, X.-Y.; Bell, T. J.; Lawley, B.; Sims, I. M.; Tannock, G. W. Substrate Use Prioritization by a Coculture of Five Species of Gut Bacteria Fed Mixtures of Arabinoxylan, Xyloglucan,  $\beta$ -Glucan, and Pectin. *Appl. Environ. Microbiol.* **2020**, *86*, e01905–19.
- (34) Li, J.; Li, S.; Zheng, Y.; Zhang, H.; Chen, J.; Yan, L.; Ding, T.; Linhardt, R. J.; Orfila, C.; Liu, D.; Ye, X.; Chen, S. Fast preparation of rhamnogalacturonan I enriched low molecular weight pectic polysaccharide by ultrasonically accelerated metal-free Fenton reaction. *Food Hydrocolloids* **2019**, *95*, 551–561.
- (35) Chen, J.; Cheng, H.; Wu, D.; Linhardt, R. J.; Zhi, Z.; Yan, L.; Chen, S.; Ye, X. Green recovery of pectic polysaccharides from citrus canning processing water. *J. Cleaner Prod.* **2017**, *144*, 459–469.
- (36) Fadrosh, D. W.; Ma, B.; Gajer, P.; Sengamalay, N.; Ott, S.; Brotman, R. M.; Ravel, J. An improved dual-indexing approach for multiplexed 16S rRNA gene sequencing on the Illumina MiSeq platform. *Microbiome* **2014**, *2*, 6.
- (37) Benjamini, Y.; Krieger, A. M.; Yekutieli, D. Adaptive linear step-up procedures that control the false discovery rate. *Biometrika* **2006**, *93*, 491–507.
- (38) Canfora, E. E.; Jocken, J. W.; Blaak, E. E. Short-chain fatty acids in control of body weight and insulin sensitivity. *Nat. Rev. Endocrinol.* **2015**, *11*, 577–591.
- (39) Tanaka, H.; Kakiyama, T.; Takahara, K.; Yamauchi, M.; Tanaka, M.; Sasaki, J.; Taniguchi, T.; Matsuo, H.; Shindo, M. The Association Among Fat Distribution, Physical Fitness, and the Risk Factors of Cardiovascular Disease in Obese Women. *Obes. Res.* **1995**, *3*, 649S–653S.
- (40) Odegaard, J. I.; Chawla, A. Pleiotropic Actions of Insulin Resistance and Inflammation in Metabolic Homeostasis. *Science* **2013**, *339*, 172–177.
- (41) Cani, P. D.; Amar, J.; Iglesias, M. A.; Poggi, M.; Knauf, C.; Bastelica, D.; Neyrinck, A. M.; Fava, F.; Tuohy, K. M.; Chabo, C.; Waget, A.; Delmee, E.; Cousin, B.; Sulpice, T.; Chamontin, B.; Ferrieres, J.; Tanti, J.-F.; Gibson, G. R.; Casteilla, L.; Delzenne, N. M.; Alessi, M. C.; Burcelin, R. Metabolic Endotoxemia Initiates Obesity and Insulin Resistance. *Diabetes* **2007**, *56*, 1761–1772.
- (42) Weisberg, S. P.; McCann, D.; Desai, M.; Rosenbaum, M.; Leibel, R. L.; Ferrante, A. W. Obesity is associated with macrophage accumulation in adipose tissue. *J. Clin. Invest.* **2003**, *112*, 1796–1808.
- (43) Wang, W.; Seale, P. Control of brown and beige fat development. *Nat. Rev. Mol. Cell Biol.* **2016**, *17*, 691–702.
- (44) Tilg, H.; Zmora, N.; Adolph, T. E.; Elinav, E. The intestinal microbiota fuelling metabolic inflammation. *Nat. Rev. Immunol.* **2020**, *20*, 40–54.
- (45) Mortensen, P. B.; Holtug, K.; Rasmussen, H. S. Short-Chain Fatty Acid Production from Mono- and Disaccharides in a Fecal Incubation System: Implications for Colonic Fermentation of Dietary Fiber in Humans. *J. Nutr.* **1988**, *118*, 321–325.
- (46) Li, S.; Li, M.; Yue, H.; Zhou, L.; Huang, L.; Du, Z.; Ding, K. Structural elucidation of a pectic polysaccharide from *Fructus Mori* and its bioactivity on intestinal bacteria strains. *Carbohydr. Polym.* **2018**, *186*, 168–175.
- (47) Onumpai, C.; Kolida, S.; Bonnin, E.; Rastall, R. A. Microbial utilization and selectivity of pectin fractions with various structures. *Appl. Environ. Microbiol.* **2011**, *77*, 5747–5754.

- (48) Ndeh, D.; Gilbert, H. J. Biochemistry of complex glycan depolymerisation by the human gut microbiota. *FEMS Microbiol. Rev.* **2018**, *42*, 146–164.
- (49) Everard, A.; Lazarevic, V.; Gaia, N.; Johansson, M.; Ståhlman, M.; Backhed, F.; Delzenne, N. M.; Schrenzel, J.; François, P.; Cani, P. D. Microbiome of prebiotic-treated mice reveals novel targets involved in host response during obesity. *ISME J.* **2014**, *8*, 2116–2130.
- (50) Rosshart, S. P.; Vassallo, B. G.; Angeletti, D.; Hutchinson, D. S.; Morgan, A. P.; Takeda, K.; Hickman, H. D.; McCulloch, J. A.; Badger, J. H.; Ajami, N. J.; Trinchieri, G.; Pardo-Manuel de Villena, F.; Yewdell, J. W.; Rehmann, B. Wild Mouse Gut Microbiota Promotes Host Fitness and Improves Disease Resistance. *Cell* **2017**, *171*, 1015–1028.e13.
- (51) Zhao, Q.; Elson, C. O. Adaptive immune education by gut microbiota antigens. *Immunology* **2018**, *154*, 28–37.
- (52) Li, S.; Li, J.; Mao, G.; Wu, T.; Hu, Y.; Ye, X.; Tian, D.; Linhardt, R. J.; Chen, S. A fucoidan from sea cucumber *Pearsonothuria graeffei* with well-repeated structure alleviates gut microbiota dysbiosis and metabolic syndromes in HFD-fed mice. *Food Funct.* **2018**, *9*, 5371–5380.
- (53) Pfeiffer, N.; Desmarchelier, C.; Blaut, M.; Daniel, H.; Haller, D.; Clavel, T. *Acetatifactor muris* gen. nov., sp. nov., a novel bacterium isolated from the intestine of an obese mouse. *Arch. Microbiol.* **2012**, *194*, 901–907.
- (54) Biagi, E.; Nylund, L.; Candela, M.; Ostan, R.; Bucci, L.; Pini, E.; Nikkila, J.; Monti, D.; Satokari, R.; Franceschi, C.; Brigidi, P.; De Vos, W. Through Ageing, and Beyond: Gut Microbiota and Inflammatory Status in Seniors and Centenarians. *PLoS One* **2010**, *5*, No. e10667.
- (55) Reijnders, D.; Goossens, G. H.; Hermes, G. D. A.; Neis, E. P. J. G.; van der Beek, C. M.; Most, J.; Holst, J. J.; Lenaerts, K.; Kootte, R. S.; Nieuwdorp, M.; Groen, A. K.; Olde Damink, S. W. M.; Boekschoten, M. V.; Smidt, H.; Zoetendal, E. G.; Dejong, C. H. C.; Blaak, E. E. Effects of Gut Microbiota Manipulation by Antibiotics on Host Metabolism in Obese Humans: A Randomized Double-Blind Placebo-Controlled Trial. *Cell Metab.* **2016**, *24*, 63–74.
- (56) Cox, L. M.; Blaser, M. J. Antibiotics in early life and obesity. *Nat. Rev. Endocrinol.* **2015**, *11*, 182–190.
- (57) Arias, L.; Goig, G. A.; Cardona, P.; Torres-Puente, M.; Diaz, J.; Rosales, Y.; Garcia, E.; Tapia, G.; Comas, I.; Vilaplana, C.; Cardona, P. J. Influence of Gut Microbiota on Progression to Tuberculosis Generated by High Fat Diet-Induced Obesity in C3HeB/FeJ Mice. *Front. Immunol.* **2019**, *10*, 2464.
- (58) Chiu, C.-M.; Huang, W.-C.; Weng, S.-L.; Tseng, H.-C.; Liang, C.; Wang, W.-C.; Yang, T.; Yang, T.-L.; Weng, C.-T.; Chang, T.-H.; Huang, H.-D. Systematic analysis of the association between gut flora and obesity through high-throughput sequencing and bioinformatics approaches. *BioMed Res. Int.* **2014**, *2014*, 906168.
- (59) Dalby, M. J.; Ross, A. W.; Walker, A. W.; Morgan, P. J. Dietary Uncoupling of Gut Microbiota and Energy Harvesting from Obesity and Glucose Tolerance in Mice. *Cell Rep.* **2017**, *21*, 1521–1533.
- (60) Zhang, C.; Abdulaziz Abbod Abdo, A.; Kaddour, B.; Wu, Q.; Xin, L.; Li, X.; Fan, G.; Teng, C. Xylan-oligosaccharides ameliorate high fat diet induced obesity and glucose intolerance and modulate plasma lipid profile and gut microbiota in mice. *J. Funct. Foods* **2020**, *64*, 103622.
- (61) Li, W.; Zhang, K.; Yang, H. Pectin Alleviates High Fat (Lard) Diet-Induced Nonalcoholic Fatty Liver Disease in Mice: Possible Role of Short-Chain Fatty Acids and Gut Microbiota Regulated by Pectin. *J. Agric. Food Chem.* **2018**, *66*, 8015–8025.
- (62) Mao, B.; Li, D.; Zhao, J.; Liu, X.; Gu, Z.; Chen, Y. Q.; Zhang, H.; Chen, W. Metagenomic Insights into the Effects of Fructo-oligosaccharides (FOS) on the Composition of Fecal Microbiota in Mice. *J. Agric. Food Chem.* **2015**, *63*, 856–863.
- (63) Kong, C.; Gao, R.; Yan, X.; Huang, L.; Qin, H. Probiotics improve gut microbiota dysbiosis in obese mice fed a high-fat or high-sucrose diet. *Nutrition* **2019**, *60*, 175–184.
- (64) Tang, D.; Wang, Y.; Kang, W.; Zhou, J.; Dong, R.; Feng, Q. Chitosan attenuates obesity by modifying the intestinal microbiota and increasing serum leptin levels in mice. *J. Funct. Foods* **2020**, *64*, 103659.
- (65) Yang, J.; Bindels, L. B.; Segura Munoz, R. R.; Martinez, I.; Walter, J.; Ramer-Tait, A. E.; Rose, D. J. Disparate Metabolic Responses in Mice Fed a High-Fat Diet Supplemented with Maize-Derived Non-Digestible Feruloylated Oligo- and Polysaccharides Are Linked to Changes in the Gut Microbiota. *PLoS One* **2016**, *11*, No. e0146144.
- (66) Cui, J.; Mai, G.; Wang, Z.; Liu, Q.; Zhou, Y.; Ma, Y.; Liu, C. Metagenomic Insights Into a Cellulose-Rich Niche Reveal Microbial Cooperation in Cellulose Degradation. *Front Microbiol* **2019**, *10*, 618.
- (67) Loy, A.; Pfann, C.; Steinberger, M.; Hanson, B.; Herp, S.; Brugioux, S.; Gomes Neto, J. C.; Boekschoten, M. V.; Schwab, C.; Urich, T.; Ramer-Tait, A. E.; Rattei, T.; Stecher, B.; Berry, D. Lifestyle and Horizontal Gene Transfer-Mediated Evolution of *Mucispirillum schaedleri*, a Core Member of the Murine Gut Microbiota. *mSystems* **2017**, *2*, e00171–16.
- (68) Lennon, G.; Balfe, Á.; Bambury, N.; Lavelle, A.; Maguire, A.; Docherty, N. G.; Coffey, J. C.; Winter, D. C.; Sheahan, K.; O'Connell, P. R. Correlations between colonic crypt mucin chemotype, inflammatory grade and *Desulfovibrio* species in ulcerative colitis. *Colorectal Dis.* **2014**, *16*, O161–O169.
- (69) Kolodziejczyk, A. A.; Zheng, D.; Elinav, E. Diet-microbiota interactions and personalized nutrition. *Nat. Rev. Microbiol.* **2019**, *17*, 742–753.
- (70) Li, G.; Xie, C.; Lu, S.; Nichols, R. G.; Tian, Y.; Li, L.; Patel, D.; Ma, Y.; Brouwer, C. N.; Yan, T.; Krausz, K. W.; Xiang, R.; Gavrilo, O.; Patterson, A. D.; Gonzalez, F. J. Intermittent Fasting Promotes White Adipose Browning and Decreases Obesity by Shaping the Gut Microbiota. *Cell Metab.* **2017**, *26*, 672–685.e4.
- (71) Seale, P. Transcriptional Regulatory Circuits Controlling Brown Fat Development and Activation. *Diabetes* **2015**, *64*, 2369–2375.